Published in final edited form as:
*J Magn Reson Imaging*. 2013 November ; 38(5): . doi:10.1002/jmri.24020.

# Simultaneous Magnetic Resonance Angiography and Perfusion (MRAP) Measurement: Initial Application in Lower Extremity Skeletal Muscle

**Katherine L. Wright, BS**[1,2], **Nicole Seiberlich, PhD**[1], **John A. Jesberger, BS**[2], **Dean A. Nakamoto, MD**[3], **Raymond F. Muzic Jr., PhD**[3,2,1], **Mark A. Griswold, PhD**[3,2,1], and **Vikas Gulani, MD, PhD**[3,2,1]

[1]Department of Biomedical Engineering, Case Western Reserve University, Cleveland, Ohio

[2]Case Center for Imaging Research, Case Western Reserve University and University Hospitals Case Medical Center, Cleveland, Ohio

[3]Department of Radiology, University Hospitals Case Medical Center, Cleveland, Ohio

## Abstract

**Purpose—**To obtain a simultaneous 3D MR Angiography and Perfusion (MRAP) using a single acquisition, and to demonstrate MRAP in the lower extremities. A time-resolved contrast-enhanced exam is utilized in MRAP to simultaneously acquire a contrast-enhanced MR angiography (MRA) and dynamic contrast-enhanced (DCE) perfusion, which currently requires separate acquisitions and thus two contrast doses. MRAP can be used to assess large and small vessels in vascular pathologies such as peripheral arterial disease.

**Materials and Methods—**MRAP was performed on ten volunteers following unilateral plantar flexion exercise (one leg exercised and one rested) on two separate days. Data were acquired after administration of a single dose of contrast agent using an optimized sampling strategy, parallel imaging, and partial-Fourier acquisition to obtain a high spatial resolution, 3D-MRAP frame every four seconds. Two radiologists assessed MRAs for image quality, a signal-to-noise ratio (SNR) analysis was performed, and pharmacokinetic modeling yielded perfusion ($K^{trans}$).

**Results—**MRA images had high SNR and radiologist-assessed diagnostic quality. Mean $K^{trans}$±standard error were 0.136±0.009, 0.146±0.012, and 0.191±0.012 $min^{-1}$ in the resting tibialis anterior, gastrocnemius, and soleus, respectively, which significantly increased with exercise to 0.291±0.018, 0.270±0.019, and 0.338±0.022 $min^{-1}$. Bland-Altman analysis showed good repeatability.

**Conclusion—**MRAP provides simultaneous high-resolution MRA and quantitative DCE exams to assess large and small vessels with a single contrast dose. Application in skeletal muscle shows quantitative, repeatable perfusion measurements, and the ability to measure physiological differences.

### Keywords

MR Angiography; Dynamic Contrast Enhanced MRI; Perfusion

Address correspondence to: Katherine Wright, University Hospitals Case Medical Center, Bolwell Building, B140, 11100 Euclid Avenue, Cleveland, OH, USA 44106, 216-844-3916, 216-844-8062 (FAX), kls115@case.edu.

## INTRODUCTION

Vascular pathologies can affect large and small vessels, and can manifest as perfusion deficits from downstream effects of large vessel disease or directly from small vessel disease. Thus, for comprehensive vascular evaluation, both large and small vessels should be assessed. Magnetic Resonance Angiography (MRA) depicts large arteries and has been widely used to assess arterial pathology (1–4). However, the microvasculature cannot be assessed on MRA images, as the spatial resolution is insufficient to depict sub-millimeter vessels. Instead, quantitative perfusion measurements provide evaluation of the microvasculature as an aggregate over the voxel volume. MR perfusion measurements are most commonly performed using dynamic contrast-enhanced (DCE) techniques (5–7), in which pharmacokinetic analysis of the administered contrast agent is used to quantify perfusion. With these techniques, noninvasive vascular MR imaging, specifically MRA and DCE MRI perfusion, can be used to separately assess the macro-and microvasculature. For example, perfusion has been used along with renal MR angiography to grade the effect of renal artery stenosis on parenchymal perfusion using two gadolinium injections (8). Since most MRA and perfusion exams each use a separate, full-dose contrast bolus, the two studies may need to be performed on different days to avoid contamination of the second exam and contrast double-dosing. These factors effectively preclude the use of MRI to evaluate both microvascular and macrovascular components of disease simultaneously. Thus, the multifactorial etiologies of vascular pathologies such as peripheral arterial disease (PAD) have been incompletely explored.

Time-resolved magnetic resonance angiography (trMRA) techniques are performed by acquiring 3D images at several time points to dynamically visualize arterial anatomy at different phases of contrast arrival. These images also contain high spatial resolution data on tissue enhancement. In this study, it was hypothesized that this tissue enhancement can be used for direct, quantitative, DCE perfusion analysis. However, trMRA image acquisitions are optimized for visualizing vascular anatomy and not DCE analysis. The challenge in a simultaneous approach is maintaining high spatial resolution needed to visualize the vasculature while also achieving high temporal resolution and sufficient tissue signal-to-noise ratio (SNR) to accurately capture changes in contrast agent concentration needed to estimate perfusion. In this study, a technique is introduced (MR Angiography and Perfusion, MRAP), which attempts to meet the stringent needs of both exams. By simultaneously acquiring angiography images and calculating a quantitative perfusion parameter, MRAP accomplishes both small and large vessel assessment in a single exam and contrast dose. MRAP is applied in the legs, and the feasibility of robustly acquiring both an MRA and measuring quantitative physiological perfusion differences are demonstrated in asymptomatic volunteers.

## MATERIALS AND METHODS

### Study Participants

In this IRB-approved, HIPAA compliant study, experiments were performed on asymptomatic, non-smoking volunteers after written informed consent. Ten volunteers participated (male/female 5/5, age 26.3±10.4 years, and weight 77.9±17.2 kg).

### Study Protocol

Each subject performed unilateral plantar flexion exercise using a resistance band for three minutes while in the MR scanner, creating a physiological perfusion difference between legs. The contralateral leg remained at rest to serve as a baseline comparison. An underlying assumption was that resting perfusion in both legs without exercise would be similar, and

therefore differences in perfusion between legs after unilateral exercise would be due to the stimulus. This can be expected to be true in asymptomatic volunteers. Imaging was initiated immediately after exercise. The experiment was performed on each subject on two separate days at least one week apart to study repeatability of the MRAP perfusion measurement. The leg that was exercised was randomly selected, and the volunteer exercised the same leg on both days.

## Image Acquisition

Imaging was performed at 3.0T (Magnetom Verio, Siemens Healthcare, Erlangen, Germany) with a peripheral angiography matrix coil and spinal array coil. Prior to exercise and the MRAP exam, a baseline $T_1$ measurement was performed using an inversion recovery experiment (9) with the following parameters: TurboFLASH; TR/TE 5s/1.33–1.39ms; flip angle 8°; inversion times 150–2000 ms.

To maintain high spatial resolution and 3D coverage while achieving high temporal resolution, a view-sharing method known as Time-resolved angiography With Interleaved Stochastic Trajectories (TWIST) was employed (2). TWIST utilizes differential sampling of central and outer regions of k-space (referred to as “A” and “B” regions, respectively) with a sliding window reconstruction, and can be combined with partial Fourier acquisition and parallel imaging to generate time-resolved angiographic images with high spatial and temporal resolution. These parameters were optimized via simulation and experiment to make the acquisition more sensitive to perfusion changes in the muscle while preserving MRA quality. The obtained settings were: A region 20%, B region 33%, GRAPPA factor 2 in the phase encoding and partition directions, and partial Fourier 6/8 along the phase encoding direction (10). The flip angle of 10° was chosen for MRAP to balance the optimal flip angle for tissue signal for the perfusion measurement and contrast-enhanced blood signal for the MRA. The TWIST sampling parameters (A and B region) were chosen based on a simulation-based exploration of these parameters and their effects on image quality (11). Optimized parameters were used for all MRAP experiments.

Contrast-enhanced MRAP exams were performed on volunteers after administration of 0.1 mmol/kg Gd-DTPA (Magnevist; Bayer, Berlin, Germany) followed by 25 ml saline at 3 ml/s. The injection of contrast was initiated approximately 2 min after cessation of exercise, following collection of pre-injection baseline images. Other MRAP imaging parameters were: TR/TE 2.97/1.48ms; resolution: $1.34\times1.6\times1.5$ $mm^3$; 90 temporal repetitions; and FOV $430\times403\times96$ $mm^3$. The acquisition time for each frame was 3.99 s, which is within the suggested range for analyzing muscle tissue enhancement curves in the lower extremities (12) and also sufficiently fast for diagnostic MRA in the legs (13).

## Evaluation of Angiography Images

Because a combined method such as MRAP may result in two suboptimal exams, both the angiographic and perfusion exams were analyzed to ensure that the technique could provide high quality MRA images while also providing perfusion information. To analyze MRA images, SNR measurements were made. As SNR values in images processed using techniques such as parallel imaging are not uniform across the image, SNR calculations cannot be made using spatially-varying regions-of-interest (ROIs) (14). Instead, the SNR at baseline was measured by taking the ratio of signal in the popliteal artery averaged over the pre-contrast images and the averaged noise over the same ROI obtained from serial baseline subtraction images. An SNR in the maximally enhanced popliteal artery was also obtained as a ratio of the signal at maximal enhancement in the same ROI to the noise as obtained from baseline measurements. Additionally, two MR-trained attending radiologists were asked to rate their confidence level for assessing lumen patency (0–100%) in the MRAP

exam in the right and left legs for the popliteal, anterior tibial, posterior tibial, and peroneal arteries.

## Perfusion Measurement

Perfusion calculations were performed offline using MATLAB (The MathWorks, Natick, Massachusetts). Time courses of signal intensity in the muscle were generated over 13.4×16 $mm^2$ (10 $voxels^2$) ROIs in three muscle groups: the tibialis anterior, soleus, and gastrocnemius. ROIs were placed centrally within the muscle group in a single axial slice.

As mentioned previously, the intrinsic $T_1$ of the tissue was measured using an inversion recovery experiment, allowing for the calculation of concentration of contrast agent (9). To convert signal intensity values from the MRAP exam to concentration, the following equation was used (9):

$$\frac{1}{T_1}=\frac{1}{T_{1,o}}+rC, \quad [1]$$

where $T_{1,o}$ is the intrinsic $T_1$ of the tissue, $T_1$ is its shortened value in the presence of contrast agent, $r$ is the relaxivity of the contrast agent, and $C$ is the concentration of the contrast agent. $T_{1,o}$ was measured prior to the MRAP exam, and $T_1$ was computed using MRAP signal values and the FLASH signal intensity relationship (9).

Gadolinium-based contrast agents are known to passively diffuse between the vascular space and the extravascular, extracellular space (EES) and are excluded from the intracellular space. The pharmacokinetics of Gd-DTPA can be described by a one compartment model with the following equation (5):

$$\frac{dc_t}{dt}=K^{trans}c_p-k_{ep}c_t, \quad [2]$$

where $c_p$ is the concentration of contrast agent in the plasma, $c_t$ is the concentration of contrast agent in the tissue, and $K^{trans}$ and $k_{ep}$ are rate constants. The time-varying concentration $c_p$ was obtained by measuring the arterial input function (AIF) in a region of interest selected within the popliteal artery. The AIF signal time-course was then fit to a gamma variate function (15,16). For both exercise and rested muscle, this study assumes flow-limited conditions, i.e., high permeability and low flow. In this case (5), the transfer constant is a function of perfusion ($F$), density ($\rho$), and hematocrit ($Hct$):

$$K^{trans}=F\rho(1-Hct), \quad [3]$$

assuming a $\rho$ of 1.05 kg/l and $Hct$ of 0.4.

Using these equations, the tissue compartment signal can be converted to contrast agent concentration (Eq 1) and can then be modeled using Equation 2 to yield fitted parameters $k_{ep}$ and $K^{trans}$ (and by extension, $F$). As established in prior studies, $K^{trans}$ is a direct quantitative measure of perfusion (5). A nonlinear least squares fit was used to estimate $k_{ep}$ and $K^{trans}$.

In addition to the ROI perfusion analysis, pixelwise perfusion maps were also generated. Due to SNR considerations, this was performed at a lower spatial resolution by down-sampling to double the voxel size (to 2.7×3.2×3 $mm^3$), and spatial and temporal averaging filters were applied (using 2×2 spatial and a three-point temporal convolution kernel with uniform weighting, respectively).

The accuracy of the measured $K^{trans}$ is dependent on the SNR of the DCE and $T_1$ quantification acquisitions. Simulations were performed to estimate the propagated error in measured $K^{trans}$ caused by noise in the image acquisition. The noise in the $T_1$ mapping was quantified by measuring the standard deviation of $T_1$ over 10 repetitions. Noise in the DCE-MRI acquisition was quantified from the first 30 frames acquired prior to contrast injection. After quantification of the SNR for both acquisitions, Monte Carlo simulations were performed by adding normally distributed random noise to an 'ideal' enhancement curve and the resulting data were fit using the modeling process described above. The ideal arterial enhancement data were generated using a fitted AIF from a volunteer scan, and the ideal muscle enhancement data were generated using known $k_{ep}$ and $K^{trans}$ values. These simulations estimate the propagated error in measured $K^{trans}$ caused by noise from image acquisition. Physiological variation in measured $K^{trans}$ was estimated as the standard deviation in the measured $K^{trans}$ in each muscle over the 10 subjects.

### Statistical Analysis

The significance of the effect of exercise on $K^{trans}$ was evaluated using a paired t-test ($\alpha$=0.05, two-tailed). The Bland-Altman method was used to compare intrasubject variability between the two imaging sessions (17). Good agreement between measurements on separate days indicates repeatability across the two days. Bland Altman analysis was performed for each muscle group (ROI measurements) at rest and after exercise across the two scanning sessions.

## RESULTS

3D MRAP images were acquired for all volunteers. Maximum Intensity Projection (MIPs) images generated after baseline subtraction are displayed in Figure 1 from three representative datasets. MRA images yielded an SNR values of 38±8 at baseline and 110±28 at peak enhancement. A summary of the results of the radiologists' assessments of the angiographic images is presented in Table 1. These results showed a high confidence in the evaluation of the angiographic images, i.e., a score approaching 100 for the confidence level of assessing lumen patency.

Figure 2 shows a representative ROI signal intensity time series and model fits for both the AIF (Figure 2a) and the gastrocnemius (Figure 2b) of exercising and resting legs in a single volunteer. Note the exercised muscle shows both a higher rate of signal change during contrast arrival, and an increased difference in signal intensity between baseline and plateau.

In Table 2, perfusion measurements are summarized for each muscle at rest and after exercise. The paired t-test results show a strong effect of exercise on $K^{trans}$ with $p$=0.008, <0.0001, and <0.0001 in the tibialis anterior, gastrocnemius, and soleus, respectively.

Bland-Altman plots are shown in Figure 3. No point falls outside two standard deviations of mean measured differences in $K^{trans}$ for soleus (Figure 3c and 3f), and one point for each of the rested and exercised muscles analyzed falls outside the limits of agreement in the Bland-Altman plots for gastrocnemius and tibialis anterior (Figure 3a,b,d,e).

Coronal and axial slices from a 3D $K^{trans}$ perfusion map are shown in Figure 4 for a volunteer whose right leg was exercised. For ease of viewing, pixels outside of the body and those in fat and solid bone structures have been removed by thresholding and manual segmentation. The resulting higher perfusion in the exercised leg is clearly seen as higher $K^{trans}$ values in the right leg compared to the rested left leg. For reference, the source images for both slices are shown in Figure 4. These images also demonstrate typical image quality and resolution.

## DISCUSSION

This study demonstrates the feasibility of the MRAP technique, which allows for the simultaneous acquisition of three-dimensional trMRA images and DCE perfusion measurements with a single gadolinium dose. While non-contrast techniques are available for both MRA and for perfusion (18–23), these are less robust than contrast-enhanced techniques, and in the case of perfusion, these are often performed on single, thick slices, limiting the clinical applicability. It follows that currently contrast-enhanced MRA and perfusion methods have found much more widespread clinical use in many applications (7).

The MRA images from MRAP maintain high SNR and were rated highly for lumen assessment by both radiologists, indicating that MRA examination quality was high for the MRAP experiments. The measurement standard error in $K^{trans}$ (perfusion) due to image noise was in the range of 6–8% of the measured $K^{trans}$, and is much smaller than the physiological variation in perfusion at rest and with exercise. The large physiological variation in perfusion across the volunteer population is likely due to factors such as the subject's effort during exercise, activity level prior to imaging, caffeine intake, and fitness level, which were not controlled in this study. The temporal resolution of approximately 4 s/volume was sufficient for accurate characterization of the tissue enhancement curves as previously described by Lutz et al. (12). While a better temporal resolution may be desirable for AIF characterization, Monte Carlo simulations (not included for brevity) showed that when modeling the AIF with a gamma variate function, the temporal resolution used here provided sufficient accuracy for estimating $K^{trans}$ given both the physiology of the lower extremities and the injection protocol used here. Model fits also showed low residual errors between the model and the obtained data for both the AIF and the time course in the muscle.

Previous MR perfusion studies have been performed in skeletal muscle using contrast-enhanced and non-contrast methods (12,24–27). The resting perfusion measurements reported here (22 – 30 ml/(100 g·min)) are in close agreement with those reported when using arterial spin labeling (24,25), which show a range between 20 and 30 ml/(100 g·min)). Lutz et al. reported DCE perfusion measurement in human skeletal muscle in resting and post-ischemic hyperemic conditions (12). The resting perfusion values in that study (median values of 4.7–5.6 ml/100 g·min) were much smaller than the measurements reported here and elsewhere (24,25), while the measurements in post-ischemic reactive hyperemia (25.4–26.7 ml/100 g·min) were similar to those after exercise in this study. The discrepancy in measurements at rest between Lutz et al. and the current study may relate to differences in the two study designs (contralateral legs being exercised versus post ischemic hyperemic), and uncontrolled effects such as exercise and caffeine intake. Measurements during near maximal post-ischemic hyperemic conditions have also been reported by Thompson et al. (102–208 ml/100 g*min) (27), which are larger than those by Lutz et al., or the exercise conditions reported here. The reason for these differences is not clear.

Perfusion in the exercised leg was significantly greater than in the non-exercised leg, demonstrating the ability of MRAP to quantify physiological perfusion differences. The perfusion in normal volunteers increased by a factor of 2.1–2.5 between rest and exercise, which is lower than the 20 to 1 maximal flow reserve measured with ultrasound (28). This is likely due to the volunteers in the present study performing a relatively modest exercise (not exercise to exhaustion) and the two minute delay between exercise and contrast injection (during baseline data collection). The resting leg could also have slightly elevated perfusion in comparison to true rest due to cardiovascular effects from the exercise. The main limitation of this study is that the level of rest prior to performing the exercise was uncontrolled, and the effort during the exercise was not quantified. Nevertheless, the

measured perfusion of 43–53 ml/100 g·min post-exercise were similar to the post-exercise perfusion values in human skeletal muscle previously reported by several groups (24,29,30).

Assuming that the perfusion in the same volunteers is similar on two separate days, Bland-Altman analysis should show good agreement between the perfusion measurements on those two days. This was observed in each muscle group both at rest and after exercise, with at most one volunteer falling outside the 95% confidence interval commonly used to demonstrate agreement between two measurements. Thus, these data indicate a good repeatability for the MRAP method.

MRAP represents a significant improvement in DCE perfusion of muscle. The double use of the MRAP data means that a single gadolinium injection makes both small and large vessel evaluation possible in a single exam. This may prove to be a clinical a74nd/or investigational advantage. Even in these asymptomatic subjects, the MRAP experiments are exemplars of the possibilities opened up by this technique, in settings where 3D perfusion measurement may be of interest. For example, although MRA exams are often performed to evaluate PAD, perfusion is not routinely measured. This is also in part due to the non-robust, thick, single-slice perfusion measurements available by both non-contrast and contrast-enhanced measurements, which reduce their diagnostic utility for assessing small or spatially varying abnormalities. The data on normal volunteers are suggestive of the usefulness of a higher resolution approach. For example, the resting perfusion in the soleus muscle is higher than in tibialis anterior or gastrocnemius, and the perfusion difference due to exercise is higher in the tibialis anterior than in the gastrocnemius and soleus muscles (214% versus 185% and 178%, respectively).

In some studies, a semi-quantitative approach has been reported in which the rapid increase of the signal intensity curves in an artery (slice 1) and in muscle (slice 2) following contrast agent injection is fit to a line, and the ratio of slopes is termed the perfusion index (31,32). Using this semi-quantitative perfusion index, significant differences were seen between normal subjects and patients with PAD, showing that perfusion mapping (and thus MRAP) could be an important diagnostic tool in PAD (31,32).

The currently used contrast-enhanced, perfusion methods would require a second contrast dose and a second scanning session if both MRA and perfusion acquisitions were to be performed, adding time, cost, inconvenience, and risk of nephrogenic systemic fibrosis (33–35). Thus, although symptoms of PAD, i.e. leg weakness and claudication, result from a constellation of physiological changes secondary to reduced tissue perfusion, the clinical benefits of measuring perfusion in the setting of PAD are still relatively poorly explored. An important recent study which investigated the semi-quantitative perfusion index correlated to a 6-minute walk distance in PAD patients, indicated a relationship between disease status and perfusion (32). The results strongly suggest that high-quality perfusion measurements could be useful in the setting of PAD. As MRAP is based on a high resolution, 3D acquisition, rather than on a single, thick slice exam, regional alterations in perfusion, or changes in various muscle groups due to intervention/treatment can be better assessed based on such an acquisition. Systematic studies are needed to explore MRAP in the setting of PAD. In addition to a MRAP examination of the distal lower extremities, a MRA exam in the proximal stations may be necessary to evaluate large vessels in the proximal station. Non-contrast methods could be considered for these proximal stations. Future studies could also investigate the use of MRAP with a lower dose of contrast agent, which may allow for a proximal station MRA and a distal lower extremity MRAP exam without an increase in total contrast agent dose.

In conclusion, MRAP provides simultaneous high-resolution MRA and quantitative DCE exams to assess large and small vessels with a single contrast dose. Application in skeletal muscle shows quantitative, repeatable perfusion measurements, and the ability to measure physiological differences. While a first application of MRAP is demonstrated in skeletal muscle, the method is general and can be applied to other organs/tissues to obtain simultaneous perfusion and MRA measurements in, for example, brain or kidney. Tissue-specific factors such as necessary temporal resolution, motion correction or image registration would need to be considered and the acquisition adjusted accordingly.

## Acknowledgments

The authors would like to thank Ms. Bonnie Hami, MA (USA) for editing assistance.

Grant Support: CTSC Cleveland, NIH Multidisciplinary 1KL2RR024990, NHLBI 1 R01HL094557, 1K99EB011527, NIH Interdisciplinary Biomedical Imaging Training Program T32EB007509, Siemens Healthcare.

## References

1. Dellegrottaglie S, Sanz J, Rajagopalan S. Technology insight: Clinical role of magnetic resonance angiography in the diagnosis and management of renal artery stenosis. Nat Clin Pract Cardiovasc Med. 2006; 3(6):329–338. [PubMed: 16729011]
2. Lim RP, Shapiro M, Wang EY, Law M, Babb JS, Rueff LE, Jacob JS, Kim S, Carson RH, Mulholland TP, et al. 3D time-resolved MR angiography (MRA) of the carotid arteries with time-resolved imaging with stochastic trajectories: comparison with 3D contrast-enhanced Bolus-Chase MRA and 3D time-of-flight MRA. AJNR Am J Neuroradiol. 2008; 29(10):1847–1854. [PubMed: 18768727]
3. Prince MR, Yucel EK, Kaufman JA, Harrison DC, Geller SC. Dynamic gadolinium-enhanced three-dimensional abdominal MR arteriography. J Magn Reson Imaging. 1993; 3(6):877–881. [PubMed: 8280977]
4. Zhang H, Maki JH, Prince MR. 3D contrast-enhanced MR angiography. J Magn Reson Imaging. 2007; 25(1):13–25. [PubMed: 17154188]
5. Tofts PS, Brix G, Buckley DL, Evelhoch JL, Henderson E, Knopp MV, Larsson HBW, Lee TY, Mayr NA, Parker GJM, et al. Estimating kinetic parameters from dynamic contrast-enhanced T 1-weighted MRI of a diffusable tracer: standardized quantities and symbols. J Magn Reson Imaging. 1999; 10(3):223–232. [PubMed: 10508281]
6. Tofts PS. Modeling tracer kinetics in dynamic Gd-DTPA MR imaging. J Magn Reson Imaging. 1997; 7(1):91–101. [PubMed: 9039598]
7. Jackson, A.; Buckley, D.; Parker, G., editors. Dynamic Contrast-Enhanced Magnetic Resonance Imaging in Oncology. Heidelberg, Germany: Springer; 2005.
8. Michaely HJ, Schoenberg SO, Oesingmann N, Ittrich C, Buhlig C, Friedrich D, Struwe A, Rieger J, Reininger C, Samtleben W, et al. Renal Artery Stenosis: Functional Assessment with Dynamic MR Perfusion Measurements—Feasibility Study. Radiology. 2006; 238(2):586–596. [PubMed: 16436819]
9. Haacke, M.; Brown, R.; Thompson, M.; Venkatesan, R. Magnetic resonance imaging: physical principles & sequence design. New York: John Wiley & Sons; 1999.
10. Wright, KL.; Seiberlich, N.; Yutzy, SR.; Muzic, RF.; Griswold, MA.; Gulani, V. Parameter optimization and demonstration of simultaneous time resolved angiography and perfusion measurement in the lower extremities at rest and with exercise. Proc of the 18th Annual Meeting of the Int Soc Magn Reson Med; Stockholm, Sweden. 2010; Poster 2740
11. Song T, Laine AF, Chen Q, Rusinek H, Bokacheva L, Lim RP, Laub G, Kroeker R, Lee VS. Optimal k-space sampling for dynamic contrast-enhanced MRI with an application to MR renography. Magn Reson Med. 2009; 61(5):1242–1248. [PubMed: 19230014]
12. Lutz AM, Weishaupt D, Amann-Vesti BR, Pfammatter T, Goepfert K, Marincek B, Nanz D. Assessment of skeletal muscle perfusion by contrast medium first-pass magnetic resonance

imaging: technical feasibility and preliminary experience in healthy volunteers. J Magn Reson Imaging. 2004; 20(1):111–121. [PubMed: 15221816]

13. Sandhu GS, Rezaee RP, Wright K, Jesberger JA, Griswold MA, Gulani V. Time-resolved and bolus-chase MR angiography of the leg: branching pattern analysis and identification of septocutaneous perforators. AJR Am J Roentgenol. 2010; 195(4):858–864. [PubMed: 20858810]
14. Dietrich O, Raya JG, Reeder SB, Reiser MF, Schoenberg SO. Measurement of signal-to-noise ratios in MR images: influence of multichannel coils, parallel imaging, and reconstruction filters. J Magn Reson Imaging. 2007; 26(2):375–385. [PubMed: 17622966]
15. Feng D, Huang SC, Wang X. Models for computer simulation studies of input functions for tracer kinetic modeling with positron emission tomography. Int J Biomed Comput. 1993; 32(2):95–110. [PubMed: 8449593]
16. Orton MR, D'Arcy JA, Walker-Samuel S, Hawkes DJ, Atkinson D, Collins DJ, Leach MO. Computationally efficient vascular input function models for quantitative kinetic modelling using DCE-MRI. Phys Med Biol. 2008; 53(5):1225–1239. [PubMed: 18296759]
17. Bland JM, Altman DG. Statistical methods for assessing agreement between two methods of clinical measurement. Lancet. 1986; 1(8476):307–310. [PubMed: 2868172]
18. Detre JA, Leigh JS, Williams DS, Koretsky AP. Perfusion imaging. Magn Reson Med. 1992; 23(1):37–45. [PubMed: 1734182]
19. Williams D, Detre J, Leigh J, Koretsky A. Magnetic Resonance Imaging of Perfusion Using Spin Inversion of Arterial Water. Proc Natl Acad Sci USA. 1992; 89(1):212–216. [PubMed: 1729691]
20. Zhang W, Williams DS, Koretsky AP. Measurement of rat brain perfusion by NMR using spin labeling of arterial water: in vivo determination of the degree of spin labeling. Magn Reson Med. 1993; 29(3):416–421. [PubMed: 8383791]
21. Edelman RR, Darby DG, Warach S. Qualitative Mapping of Cerebral Blood Flow and Functional Localization with Echo-planar MR Imaging and Signal Targeting with Alternating Radio Frequency. Radiology. 1994; 192:513–520. [PubMed: 8029425]
22. Kwong KK, Chesler DA, Weisskoff RM, Donahue KM, Davis TL, Ostergaard L, Campbell TA, Rosen BR. MR perfusion studies with T1-weighted echo planar imaging. Magn Reson Med. 1995; 34(6):878–887. [PubMed: 8598815]
23. Buxton RB, Frank LR, Wong EC, Siewert B, Warach S, Edelman RR. A general kinetic model for quantitative perfusion imaging with arterial spin labeling. Magn Reson Med. 1998; 40(3):383–396. [PubMed: 9727941]
24. Elder CP, Cook RN, Chance MA, Copenhaver EA, Damon BM. Image-based calculation of perfusion and oxyhemoglobin saturation in skeletal muscle during submaximal isometric contractions. Magn Reson Med. 2010; 64(3):852–861. [PubMed: 20806379]
25. Boss A, Martirosian P, Claussen CD, Schick F. Quantitative ASL muscle perfusion imaging using a FAIR-TrueFISP technique at 3. 0 T. NMR Biomed. 2006; 19(1):125–132. [PubMed: 16404727]
26. Faranesh AZ, Kraitchman DL, McVeigh ER. Measurement of kinetic parameters in skeletal muscle by magnetic resonance imaging with an intravascular agent. Magn Reson Med. 2006; 55(5):1114–1123. [PubMed: 16598733]
27. Thompson RB, Aviles RJ, Faranesh AZ, Raman VK, Wright V, Balaban RS, McVeigh ER, Lederman RJ. Measurement of skeletal muscle perfusion during postischemic reactive hyperemia using contrast-enhanced MRI with a step-input function. Magn Reson Med. 2005; 54(2):289–298. [PubMed: 16032661]
28. Lindner JR, Womack L, Barrett EJ, Weltman J, Price W, Harthun NL, Kaul S, Patrie JT. Limb Stress-Rest Perfusion Imaging With Contrast Ultrasound for the Assessment of Peripheral Arterial Disease Severity. JACC Cardiovascular Imaging. 2008; 1(3):343–350. [PubMed: 19356447]
29. Frank LR, Wong EC, Haseler LJ, Buxton RB. Dynamic imaging of perfusion in human skeletal muscle during exercise with arterial spin labeling. Magn Reson Med. 1999; 42(2):258–267. [PubMed: 10440950]
30. Nygren A, Greitz D, Kaijser L. Skeletal muscle perfusion during exercise using Gd-DTPA bolus detection. Journal of Cardiovascular Magnetic Resonance. 2000; 2(4):263–270. [PubMed: 11545125]

31. Isbell DC, Epstein FH, Zhong X, DiMaria JM, Berr SS, Meyer CH, Rogers WJ, Harthun NL, Hagspiel KD, Weltman A, et al. Calf muscle perfusion at peak exercise in peripheral arterial disease: measurement by first-pass contrast-enhanced magnetic resonance imaging. J Magn Reson Imaging. 2007; 25(5):1013–1020. [PubMed: 17410566]

32. Anderson JD, Epstein FH, Meyer CH, Hagspiel KD, Wang H, Berr SS, Harthun NL, Weltman A, Dimaria JM, West AM, et al. Multifactorial determinants of functional capacity in peripheral arterial disease: uncoupling of calf muscle perfusion and metabolism. J Am Coll Cardiol. 2009; 54(7):628–635. [PubMed: 19660694]

33. Evenepoel P, Zeegers M, Segaert S, Claes K, Kuypers D, Maes B, Flamen P, Fransis S, Vanrenterghem Y. Nephrogenic fibrosing dermopathy: a novel, disabling disorder in patients with renal failure. Nephrology, dialysis, transplantation. 2004; 19(2):469–473.

34. Grobner T. Gadolinium – a specific trigger for the development of nephrogenic fibrosing dermopathy and nephrogenic systemic fibrosis? Nephrology, dialysis, transplantation. 2006; 21:1104–1108.

35. Kanal E, Barkovich AJ, Bell C, Borgstede JP, Bradley WG, Froelich JW, Gilk T, Gimbel JR, Gosbee J, Kanal E, et al. ACR Guidance Document for Safe MR Practices: 2007. AJR Am J Roentgenol. 2007; 188(6):1447–1474. [PubMed: 17515363]

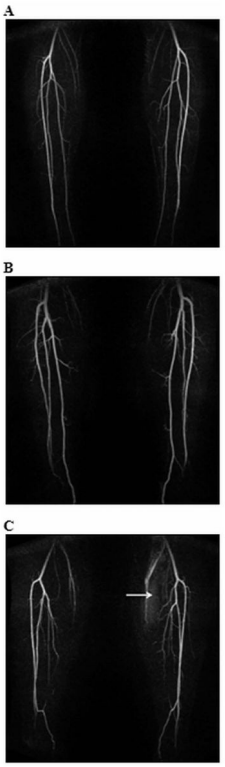


**Figure 1.**
MIPs of a single time frame from three representative trMRA exams of the distal lower extremities. The subject in Figure 1c has bilateral hypoplastic posterior tibial arteries, and peroneal continuation into the hindfoot. For this subject, note also the higher signal in left, exercised leg musculature (arrow) in this frame than in the rested leg.

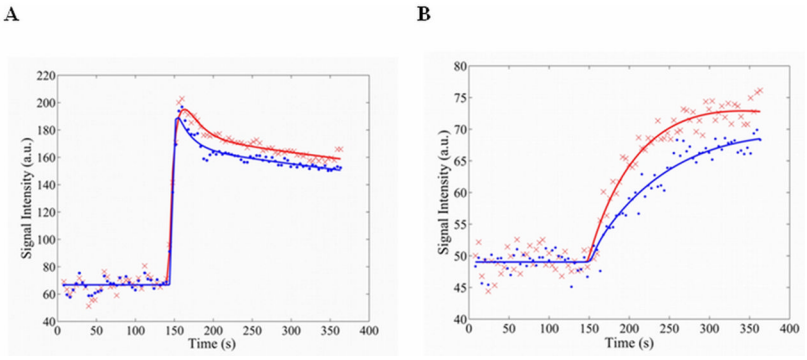


**Figure 2.**

Representative signal intensity curves and model fits for the AIF (A) and the muscle enhancement (B) in a single volunteer. Signal intensity curves were adjusted so that the mean baseline signal intensities for exercised and rested curves were equivalent for direct comparison. Red 'x' - Exercise data. Red line - Exercise model fit. Blue points - Rest data. Blue line - Rest model fit.

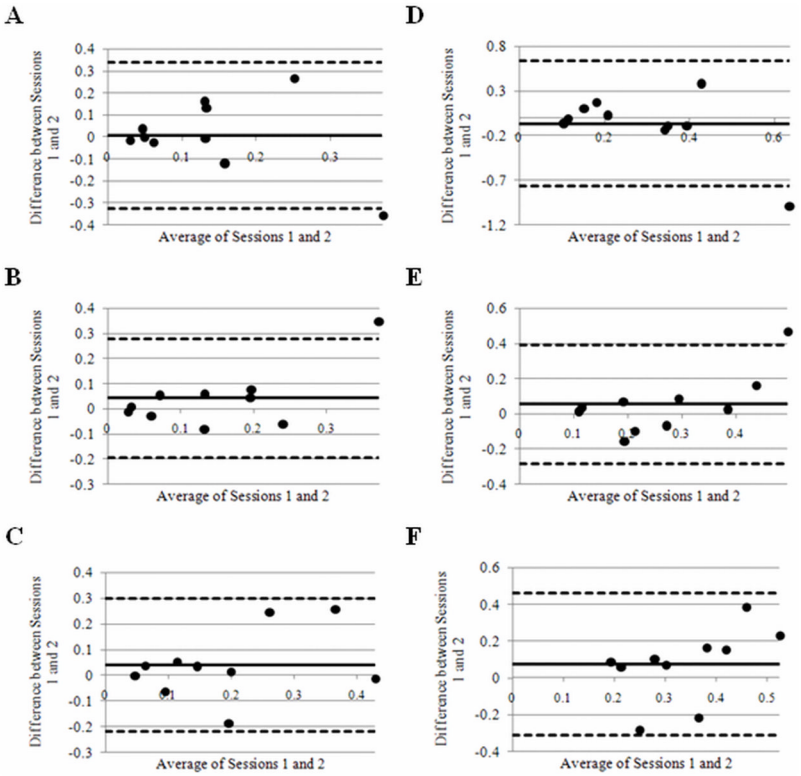


**Figure 3.**

Bland Altman plots of $K^{trans}$ in resting tibialis anterior, gastrocnemius, and soleus muscle (A, B, and C respectively) and exercised tibialis anterior, gastrocnemius, and soleus muscle (D, E, and F respectively). The solid lines represent the mean difference between sessions in all volunteers. Dashed lines represent ± 2 standard deviations from the mean.

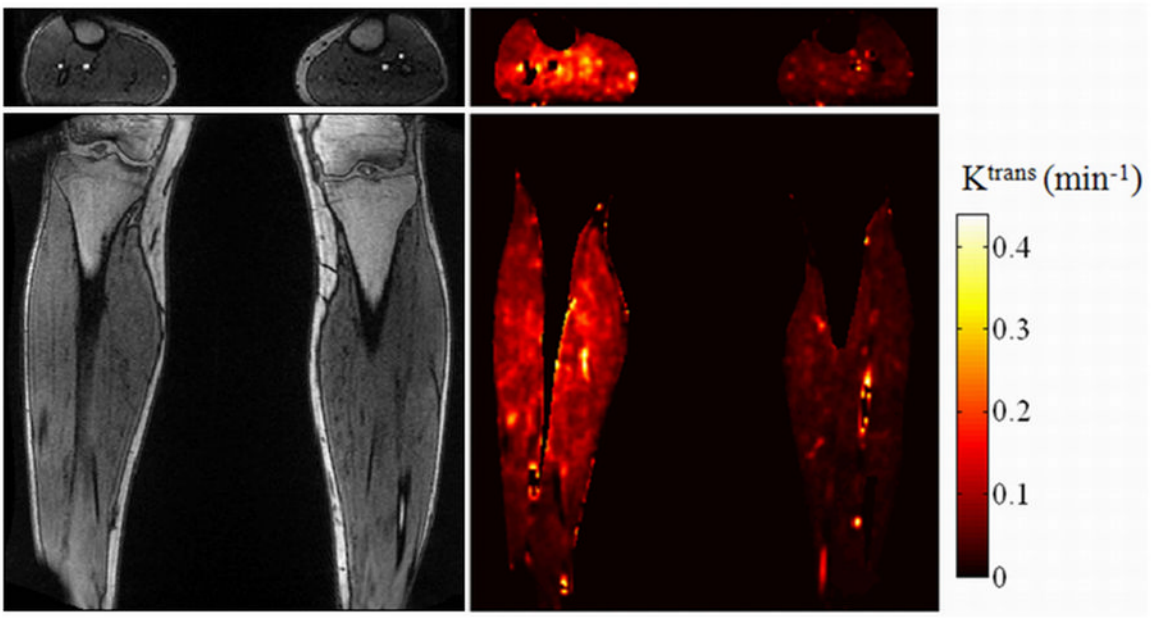


**Figure 4.**

Left column: Original axial and coronal source images corresponding to the parameter map. Right column: Pixel-wise $K^{trans}$ ($min^{-1}$) axial and coronal parameter map. The right leg was exercised while the left leg remained at rest. Note the perfusion was higher in the exercised muscle than in the rested muscle.

**Table 1**

Summary of results of radiologists' assessments of the MRA MIPs.

| | Confidence Level in Assessing Lumen Patency in Right Leg | | | | Confidence Level in Assessing Lumen Patency in Left Leg | | | |
|---|---|---|---|---|---|---|---|---|
| | **Popliteal** | **ATA** | **PTA** | **Peroneal** | **Popliteal** | **ATA** | **PTA** | **Peroneal** |
| Mean | 96% | 94% | 97% | 99% | 98% | 95% | 97% | 99% |
| Maximum | 100% | 100% | 100% | 100% | 100% | 100% | 100% | 100% |
| Minimum | 70% | 80% | 50% | 90% | 75% | 80% | 50% | 90% |

ATA, anterior tibial artery; PTA, posterior tibial artery.

**Table 2**

$K^{trans}$ ($min^{-1}$) and calculated perfusion (ml/100g/min) values for resting and exercised muscles.

| | Rest | | | | Exercise | | | |
|---|---|---|---|---|---|---|---|---|
| **Muscle** | **$K^{trans}$ ($min^{-1}$)** | **variation across subjects (std, $min^{-1}$)** | **Perfusion (ml/100g/min)** | **variation across subjects (std, ml/100g/min)** | **$K^{trans}$ ($min^{-1}$)** | **variation across subjects (std, $min^{-1}$)** | **Perfusion (ml/100g/min)** | **variation across subjects (std, ml/100g/min)** |
| Tibialis Anterior | 0.14±0.01 | 0.13 | 22±1 | 21 | 0.29±0.02 | 0.24 | 46±3 | 38 |
| Gastroc-nemius | 0.15±0.01 | 0.14 | 23±2 | 19 | 0.27±0.02 | 0.16 | 43±3 | 25 |
| Soleus | 0.19±0.01 | 0.14 | 30±2 | 22 | 0.34±0.02 | 0.15 | 54±3 | 24 |

$K^{trans}$ ($min^{-1}$) mean measurement error: from simulation evaluating noise propagation in the images. Variation across subjects: standard deviation in the measured parameter across the 10 subjects.